



Biodecolorization and biodegradation of Reactive Green 12 textile industry dye and their post-degradation phytotoxicity-genotoxicity assessments

Shweta Singh¹ · Roshan Lal Gautam¹ · Dharendra K. Chaudhary² · Devendra Singh³ · Ram Naraiyan¹

Received: 14 March 2024 / Revised: 1 May 2024 / Accepted: 5 May 2024 / Published online: 16 May 2024
© The Author(s), under exclusive licence to Springer-Verlag GmbH Germany, part of Springer Nature 2024

Abstract

The employment of versatile bacterial strains for the efficient degradation of carcinogenic textile dyes is a sustainable technology of bioremediation for a neat, clean, and evergreen globe. The present study has explored the eco-friendly degradation of complex Reactive Green 12 azo dye to its non-toxic metabolites for safe disposal in an open environment. The bacterial degradation was performed with the variable concentrations (50, 100, 200, 400, and 500 mg/L) of Reactive Green 12 dye. The degradation and toxicity of the dye were validated by high-performance liquid chromatography, Fourier infrared spectroscopy analysis, and phytotoxicity and genotoxicity assay, respectively. The highest 97.8% decolorization was achieved within 12 h. Alternations in the peaks and retentions, thus, along with modifications in the functional groups and chemical bonds, confirmed the degradation of Reactive Green 12. The disappearance of a major peak at 1450 cm^{-1} corresponding to the $-\text{N}=\text{N}-$ azo link validated the breaking of azo bonds and degradation of the parent dye. The 100% germination of *Triticum aestivum* seed and healthy growth of plants verified the lost toxicity of degraded dye. Moreover, the chromosomal aberration of *Allium cepa* root cell treatment also validated the removal of toxicity through bacterial degradation. Thereafter, for efficient degradation of textile dye, the bacterium is recommended for adaptation to the sustainable degradation of dye and wastewater for further application of degraded metabolites in crop irrigation for sustainable agriculture.

Keywords Detoxification · Biodegradation · Bacteria · Biodecolorization · Phytotoxicity · Genotoxicity

Introduction

The environmental damage resulting from the discharge of wastewater from the textile industry is an escalating global concern. The textile industry generates a substantial volume

of wastewater that contains a diverse range of chemicals, primarily complex and toxic dyes. Approximately 10,000 synthetic dyes are used in the textile industry, with a global production of 7×10^7 metric tons per year. This tremendous production and release of dyes pose a significant threat to environmental safety (Qin et al. 2016; Sampaio et al. 2018). Most importantly, dyes altogether are accountable for elevated levels of chemical oxygen demand, biological oxygen demand, and total organics when discharged into aquatic systems (Forss et al. 2017). Wherein dyes in aquatic environments can undergo chemical changes, leading to the creation of new compounds that may have different levels of toxicity compared to the original molecules (Padamavathy 2003; Buntić et al. 2017). Azo dyes are a significant component of pollution and are a widespread type of complex dyes commonly used in textile dyeing (Jadhav et al. 2011). Azo dyes are recognized as resistant to biodegradation and extremely poisonous. These compounds are extremely stable and difficult to break due to the presence of an azo bond ($-\text{N}=\text{N}-$) as the main chromophoric group (Krishnamoorthy et al. 2018).

Communicated by PANKAJ BHATT.

✉ Ram Naraiyan
ramnarain_itrc@rediffmail.com

¹ Department of Biotechnology, Faculty of Science, Veer Bahadur Singh Purvanchal University, Jaunpur, Uttar Pradesh 222003, India

² Centre for Renewable Energy, Prof. Rajendra Singh (Rajju Bhaiya) Institute of Physical Sciences for Study and Research, Veer Bahadur Singh Purvanchal University, Jaunpur, Uttar Pradesh 222003, India

³ Faculty of Biotechnology, Institute of Biosciences and Technology, Shri Ramswaroop Memorial University, Lucknow Deva Road, Barabanki, Uttar Pradesh 225001, India

Reactive dyes are classified as azo dyes because of the azo bonds, viz., Reactive Green 12 (RG12), Reactive Black 5 (RB5), Reactive Green 19 (RG19), and Reactive Yellow 2 (RY2), etc. (Hatice 2010). The abundance of such dyes and their byproducts in inadequately treated wastewater is visually unappealing and results in decreased sunlight penetration. This leads to a reduction in photosynthetic activity, dissolved oxygen levels, and water quality (Ryu et al. 2023). Additionally, it has serious detrimental impacts on aquatic plants and animals, causing significant environmental issues globally (Jadhav et al. 2011; Alsukaibi 2022). Additionally, the genotoxic, carcinogenic, and mutagenic potential of azo dyes on humans is well acknowledged (Goud et al. 2020), which requires complete degradation these days.

Over the years, various physical and chemical processes, including oxidation processes using ozone, filtration, ion exchange, adsorption, coagulation, flocculation, electrochemical treatment, Fenton, photocatalysis, and membrane processes, have been exercised to remove contaminants from the wastewater (Khan et al. 2022). Nevertheless, these methods are inefficient and produce a vast volume of harmful sludge as a secondary contaminant, causing additional environmental and community issues (Bilinska et al. 2019; Bharti et al. 2019). On the contrary, biological treatment procedures are environmentally friendly, economically efficient, sustainable, no sludge generating, and globally acceptable (Bilinska et al. 2019; Kishor et al. 2021). The employment of enzymes, bacteria, fungi, yeast, archaea, and algae to derive degradation some of them are utilized in the bioremediation of textile dyes (Peng and Guo 2020; Singh et al. 2022). Specifically, using bacteria for wastewater treatment enables the process to circumvent structural obstacles (Buntić et al. 2017). Bacteria are incredibly versatile and can adapt to a broader range of environments (Bholay et al. 2012) and are thought to be the most effective agents because of their rapid development, extensive versatility, and metabolic adaptability as compared to other microbes (Bilinska et al. 2019; Garg et al. 2020). Hence, the bacteria are preferred to execute the proper treatment and biodegradation of textile dyes and wastewater. Bacteria possess the ability to break down, remove color, remove toxins, and convert various contaminants into minerals through specific metabolic pathways (Cao et al. 2019; Kishor et al. 2021).

The first stage of bacterial degradation and decolorization involves the enzymatic breaking of azo linkages (Pandey et al. 2007; Singh et al. 2017). Azo dyes can be decolorized and degraded through enzymatic treatment, which involves the use of oxidoreductase enzymes. Laccase and azoreductase are important enzymes in this process. Laccase is a non-specific oxidase enzyme that can oxidize different aromatic compounds, while azoreductase is a specific protein that helps in reducing azo bonds. Reducing factors like NADPH and NADH enable azoreductase to effectively break

down the azo bonds and catalyze the decolorization process (Kumaran et al. 2020; Fazeliyan et al. 2021).

However, in order to address the chronic dyes and determine the cause of toxicity, whether it is due to degraded dye products or by the parent molecule itself, this is a comprehensive and wide-ranging approach. Evaluating the toxicity of pollutants and intermediates generated during their breakdown is essential for determining the feasibility of a bioremediation process. The toxicity assessment of azo dyes has been reported using several tests, such as phytotoxicity, microbiological toxicity, genotoxicity, and mutability assays, as documented by Jadhav et al. (2010) and Parshetti et al. (2010). Utilizing plants to assess the phytotoxicity and genotoxicity of both degraded and undegraded dye can be a highly cost-effective method. Furthermore, this approach can significantly promote the reuse of degraded nontoxic dye water in sustainable agriculture for the purpose of irrigation and safe disposal in the environment.

Therefore, keeping in view the facts, the current study investigated the bacterial strain *Bacillus Cereus* SSC (*B. cereus* SSC) for decolorization and degradation of RG12 dye to uncover the biological events involved in dye remediation. In addition, both the parent dye and degraded dye were tested for phytotoxicity and genotoxicity to assess the detoxification of the parent dye in terms of seed germination, seedling development, and genomic changes.

Materials and methods

Textile dye and chemicals

The textile RG12 dye ($C_{60}H_{37}Cl_3N_{16}NiO_{21}S_7 \cdot Na_6$, Mol.wt.: 1845.5 g/mol, $\lambda_{max} = 656$ nm, monoazo dye) used in the study were purchased from the Techno Color Corporation, Govandi, Mumbai (Fig. 1). The RG12 is most popularly used in the textile and carpet industries. However, all reagents used in the analyses and media constituents were of analytical grade with the highest purity (Sigma-Aldrich Chemicals Pvt. Ltd).

Bacterial strain and its maintenance

The bacterial culture (*B. cereus* SSC; ACCESSION No: LC720431) employed in the study was isolated from the textile effluent and maintained in the MTRC laboratory, V.B.S. Purvanchal University, Jaunpur, Uttar Pradesh, India (25.7464° N, 82.6837° E). The culture of bacteria was routinely grown in nutrient broth at 30 °C, and decolorization was performed in a modified dye medium (glucose 5.0 g.L⁻¹; NH₄Cl 1.5 g.L⁻¹; K₂HPO₄ 0.5 g.L⁻¹; MgSO₄ 0.1 g.L⁻¹; CaCl₂ 0.1 g.L⁻¹; and FeSO₄ 0.07 g.L⁻¹, pH 7.0) with dye for bacterial adaptation.

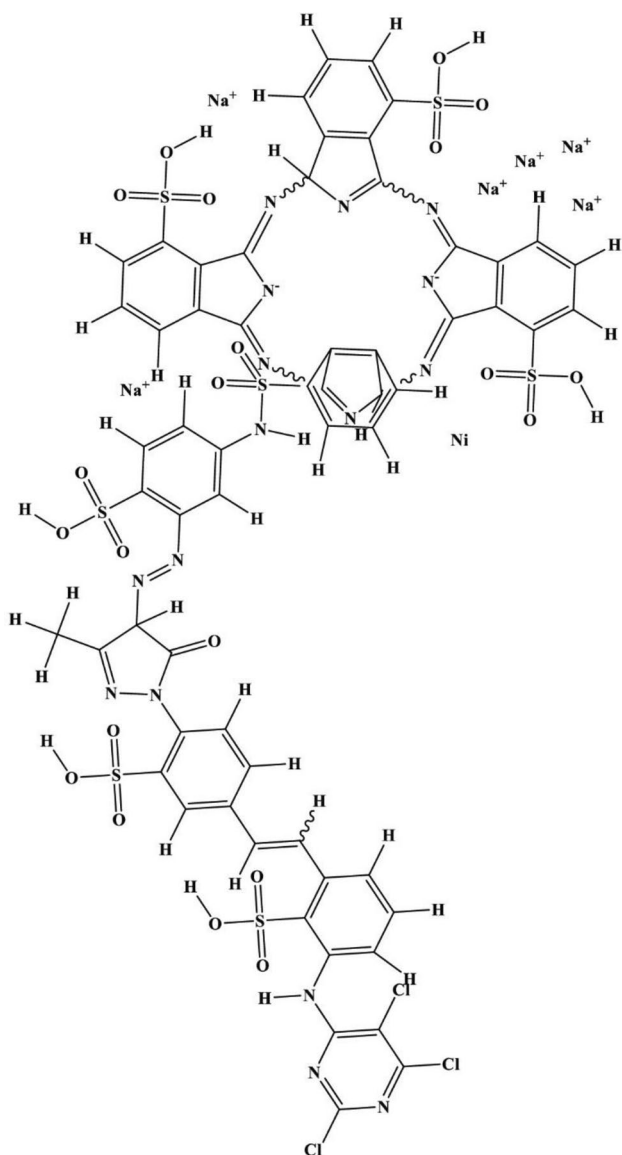


Fig.1 The molecular chemical structure of Reactive Green 12 dye used in the current study. The dye structure was drawn by using the software ChemDraw 18.1 version structured as Guendouz et al. (2013)

Biodegradation studies

Decolorization of dye was conducted in the sets of conical flasks of 100 ml size containing minimal broth media (Peptone 5.0 g, NaCl 5.0 g, Beef extract 3.0 g, water 1000 ml at pH 7.0) in different concentrations (50, 100, 200, 400, and 500 mg/L) of RG12 dye. The aliquots of dye solutions were filtered using the syringe filters (0.22 μm) and aseptically added to the sterile medium prior to bacterial inoculation. All sets were inoculated with 200 μL of bacterial inoculum and incubated BOD in an incubator at 37°C. The sets were constantly monitored, and samples were collected every half

hour. Prior to measuring the absorbance, the samples were subjected to centrifugation at 12,000g for 1 min in order to eliminate any suspended materials. All the sets run conducted in at least triplicates ($n = 3$).

The percentage of dye decolorization was calculated as below:

$$\text{Decolorization percentage (\%)} = \frac{100(Abs_{t_0} - Abs_{t_f})}{Abs_{t_0}}$$

were, Abs_{t_0} = Absorbance at the initial of culture, Abs_{t_f} = Absorbance at the end of culture.

High-performance liquid chromatography (HPLC) analysis

The textile dye (200 mg/L) analysis was conducted using an RPC-18 column (250 mm \times 4.5 mm) fitted with a dual-wavelength detector, employing the isocratic flow method. A 10 μL sample was injected for gradient elution using a mobile phase consisting of methanol and water in a ratio of 90:10 v/v. The flow rate was set at 1 mL/min, and the column temperature was maintained at 20 °C. The spectra were obtained using the Shimadzu Prominence Binary Gradient HPLC LC-20AD Pump.

Fourier transform infrared (FTIR) spectroscopy analysis.

To carry out degradation, the samples (200 mg/L) were treated with the desired bacterial inoculum. The samples taken from the degraded dye were centrifuged at 7000g for 20 min to remove bacterial cells, etc. Furthermore, the culture supernatants were collected employing an equivalent volume of ethyl acetate. Then after, the obtained samples were examined by placing a sample drop into the thin-film cell. Samples were combined in a 5:95 ratio with spectroscopically pure KBr for the FTIR analysis. The pellets were placed in a sample holder and subjected to analysis at 16 scan speeds and in the mid-IR range (400–4000 cm^{-1}) (D'Souza et al. 2017). The degraded products were analyzed using the PerkinElmer Spectrum Version (10.5.2.636) spectrometer for all FTIR investigations.

Phytotoxicity assay

The toxicity of the original and degraded RG12 dye was assessed using crop seedlings (*Triticum aestivium*) that were sterilized using 0.1% HgCl_2 (w/v) for 5 min. The assay was performed on two groups, one treated with the parent dye and the other treated with the degraded dye metabolite. The degraded dye sample was used to expose seeds and subjected to a phytotoxicity assay. However, the distilled water was

used as a control to treat the seeds and irrigation. Seeds were germinated in disinfected Petri dishes holding filter paper saturated with the equivalent aliquots of treated and degraded dye. Each treatment included subjecting the seeds to both test solutions and maintaining them at room temperature. The seed germination rate was measured after 48 h of treatment. The germinated seeds were transferred to a plastic container with cotton at the bottom as a substrate. They were then exposed to the RG12 dye, along with its degradation metabolites. The observation continued, and the assay was conducted for 15 days. The criteria, such as the percentage of seed germination, root and shoot length, total number of leaves, and shoot vigor index, had to be recorded to observe any significant alterations (Kalyani et al. 2009; Rao and Prasad 2014). The % seed germination was determined using the following formula.

$$\text{Germination percentage (\%)} = \frac{\text{No. of seeds germinated}}{\text{No. of seeds used}} \times 100$$

While the seedling vigor index (SVI) was determined as below:

$$\text{SVI} = (\text{Root length} + \text{Shoot length}) \times \% \text{ Seed germination}$$

Genotoxicity assay

The roots of *Allium cepa* were employed for the cytotoxicity assay. For the toxicity test, the roots were exposed to both parent dye solution and dye treated with bacteria. The treated fresh roots (2–2.5 cm) from both solutions were cut from the tuber using scissors. The acetocarmine was used to stain the root tips employing the meristematic squash technique (Caritá and Marin-Morales 2008; Prasad and Rao 2013; Sabeen et al. 2020). Finally, a light microscope (100X) (Magnus microscopes, model MLX) was used to recognize genetic abnormalities and chromosomal aberrations.

Statistical analysis

All study experiments were conducted in triplicate ($n = 3$), and values are mean \pm standard deviation. The data was processed using GPPS 7 and Origin Pro 8.

Result

Decolorization of parent dye

The bacterium (*B. cereus* SSC) was effectively degraded to RG12 dye and supplemented into the broth medium under static conditions. The studies on dye decolorization indicated that the dye underwent gradual degradation as the incubation

periods (ranging from 0.5 to 12 h) increased. Nevertheless, during the incubation period, the sets that were not inoculated retained their initial color without noticing any reduction. Therefore, it was evident that the bacterium had the potential to degrade the RG12 dye within a 12-h timeframe. The lower quantities of dye underwent degradation more readily, but larger concentrations required a somewhat longer duration for degradation (Fig. 2).

HPLC analysis of degraded and undegraded RG12 dye

The HPLC testing of both treated and untreated exhibited significant differences in the peaks and their retention times. The development and disappearance of distinct peaks in the degraded samples collected after 4, 8, and 12 h of incubation revealed the process of degradation. The analysis of the parent dye identified four unique peaks, including a prominent peak at a retention time of 2.784 min and three smaller peaks at retention times of 3.955, 3.072, and 3.392 min. The samples that underwent degradation after 4 h exhibited four clearly identifiable peaks with retention times of 2.662, 6.092, 7.042, and 13.503. However, the examination of samples after 8 h of incubation indicated the presence of three peaks at retention times of 4.758, 6.006, and 6.579. In addition, the dye that was treated for 12 h during analysis exhibited only a single peak at a retention time of 6.324. Furthermore, all of the significant peaks observed in the original dye were disappeared in the final samples. The observed differences in the HPLC chromatogram, characterized by distinct peaks, provide evidence for the following biotransformation and biodegradation of RG12 dye into smaller metabolites. These findings indicate that the parent dye underwent degradation after 4, 8, and 12 h of bacterial treatment. These observations also validated the bacterial degradation of RG12, as seen by the altered pattern of peaks and changes in absorbance (Fig. 3).

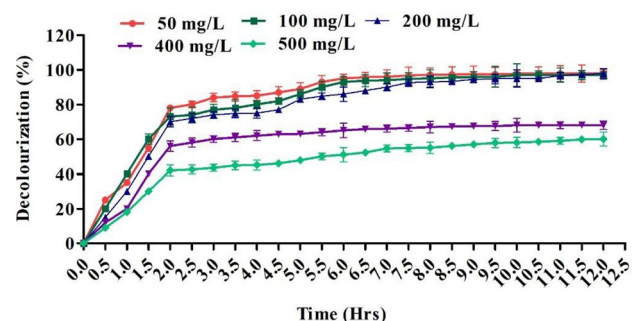


Fig. 2 Effect of different concentrations (50, 100, 200, 400 and 500 mg/L) of Reactive Green 12 on its decolorization employing a bacterium (*B. cereus* SSC)

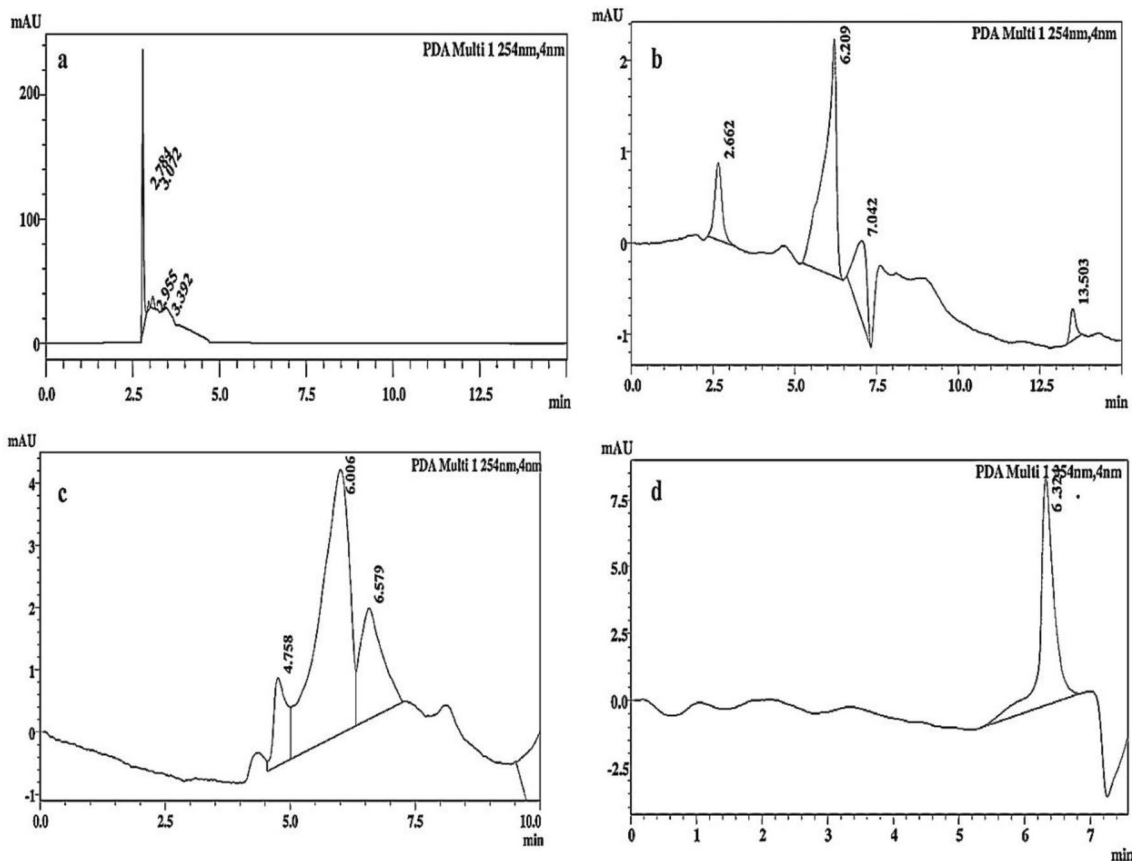


Fig. 3 HPLC Analysis: **a** Reactive Green 12; degraded metabolites by *B. cereus* SSC **b** 4 h, **c** 8 h and **d** 12 h

FTIR analysis of degraded and undegraded RG12 dye

The FTIR spectra analysis of both the parent undegraded and degraded RG12 dye revealed a varying number of peaks with different wavenumbers. The data from the degraded and undegraded dye samples were compared and interpreted, as depicted in Fig. 4 a, b, c, d, and summarized in Table 1. The undegraded RG12 dye samples exhibited peaks at 3737 and 3854 cm^{-1} , corresponding to the stretching of O–H bonds within the molecule. The undegraded parental RG12 dye samples exhibited peaks at 3737 and 3854 cm^{-1} , indicating the presence of intra-molecular hydrogen-bonded O–H stretching. The peaks detected at a wavenumber of 1620 cm^{-1} corresponded to the functional groups involved in $\text{N}\equiv\text{N}$ stretching, NH out of the plane, C=O stretch, NH_2 in the plane band, aromatic $\text{CH}=\text{CHR}$, and C=N stretching. The peak value of 3325 cm^{-1} indicated the deformation of alkane C–H bonds, the presence of RCO–OH (dimer OH) groups, the stretching of NH bonds in amines, and the asymmetric stretching of ArO–H bonds in the aromatic ring of phenol, which is a component of the original dye. The carboxylic acid O–H stretching was observed at a wavenumber

of 2361 cm^{-1} . In addition, the analysis identified a peak at 2132 cm^{-1} corresponding to the stretching of $\text{C}\equiv\text{C}$ in alkyl-substituted compounds. It also detected the stretching of R–N–C in isocyanide, N=C in R–N=C=S, and N=N=N. Furthermore, the analysis indicated the presence of Si–H silane in RG12 dye. The peak value of 1450 cm^{-1} indicates the presence of a $\text{N}=\text{N}$ azo bond. However, a signal observed at 585 cm^{-1} indicates the presence of C–Br stretching in the parent dye (Fig. 4a). Furthermore, the FTIR spectral analysis of the degraded RG12 dye revealed distinct peaks that corresponded to certain stages of dye degradation over time. The observations revealed a greater number of peaks in the damaged sample compared to the original dye. Remarkably, there was a substantial decrease in the prominent peaks of the deteriorated samples, which were essentially present in the original dye samples. Moreover, the appearance of multiple new peaks indicating the inclusion of functional groups was observed. The FTIR spectra of the deteriorated dye at 4, 8, and 12 h showed significant shifts in the peak positions compared to the original dye (RG12 dye). The absence of a prominent peak at 1450 cm^{-1} , which is specifically associated with the $\text{N}=\text{N}$ azo link, suggests the degradation and decolorization of the parent dye due to the

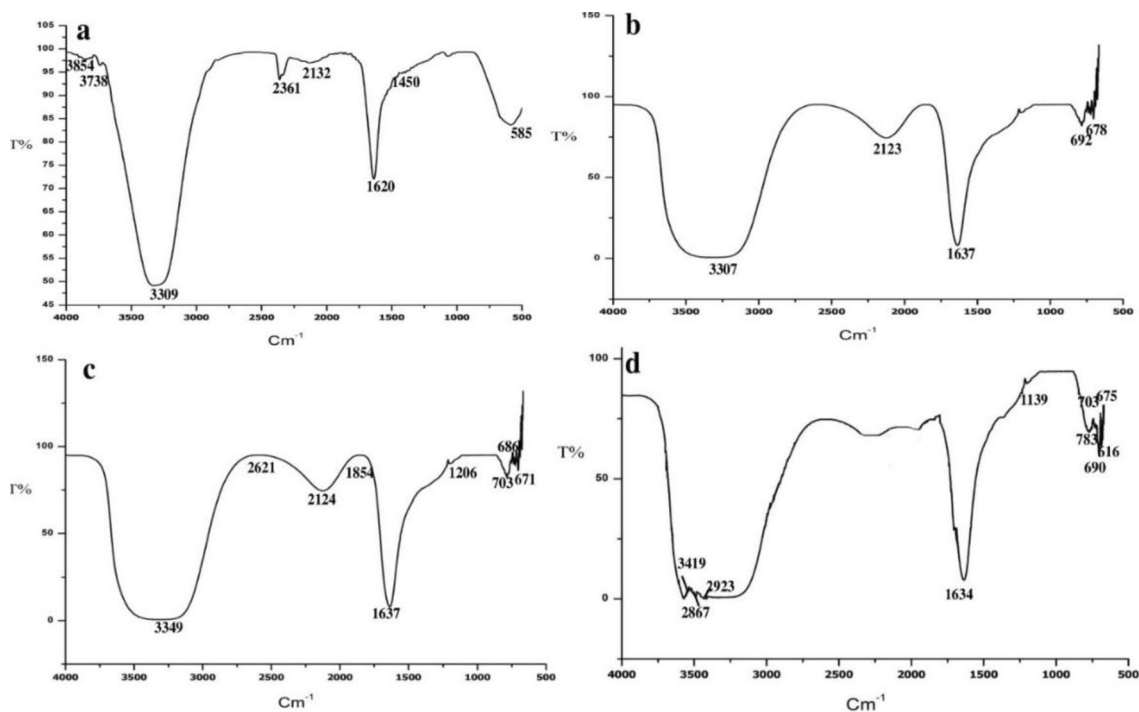


Fig. 4 FTIR analysis spectrum **a** spectrum of parent Reactive Green 12 dye **b** degraded dye at 4th h, **c** at 8th h and **d** at 12 h

breaking of azo bonds. The samples subjected to 4 h of bacterial treatment displayed peaks at 3307, 2124, 1637, 678, and 692 cm^{-1} (Fig. 4b). During the degradation process, the dye exhibited the emergence of several additional peaks after 8 h, including peaks at 3349, 2621, 2124, 1854, 1636, 1206, 703, 671, and 686 cm^{-1} (Fig. 4c). The analysis of the bacterial treatment sample collected over a 12-h period revealed distinct peaks at wavenumbers of 3419, 2923, 1634, 1407, 1139, 783, 703, 690, 675, and 616 cm^{-1} (Fig. 4d). The peaks at 3307, 3349, and 3419 cm^{-1} , which correspond to N–H and O–H stretching, were observed in the samples treated for 4, 8, and 12 h. These peaks were not present in the original dye sample. Additionally, a peak at 1634–37 cm^{-1} was observed in the treated samples. Furthermore, it was observed that the magnitudes of all peaks were diminished. Based on the observations, the sample that was taken at the 4th hour decreased from 1637 to 1636 and then further declined to 1634 during the final stage of degradation at the 12th h. The decrease in peak intensities seen in the FTIR spectrum indicates the degradation of aromatic/aliphatic nitro compound (NO_2) asymmetric and oxime stretching ($\text{C}=\text{N}-\text{OH}$). The presence of peak values at 2621–2923 cm^{-1} in degraded samples (which are not observed in the original dye) indicates the presence of aldehyde and alkane C–H stretching vibrations. The presence of isocyanide acid in the original dye is confirmed by the R–N–C and N=N=N stretching observed at 2132 cm^{-1} . In deteriorated samples, the stretching of the CS bond in sulfur-containing compounds

is observed around 675–703 cm^{-1} . The highest point of the deteriorated samples at 1139 cm^{-1} indicates the stretching of the CN bond, which confirms the existence of an amine compound after 12 h. The peak observed at 3305 cm^{-1} corresponds to the stretching vibrations of the –C–H– bonds. Furthermore, the peak at 2123 cm^{-1} corresponds to the stretching of aromatic C=C bonds and the stretching of N=C bonds in the R–N=C=S group in the deteriorated dye. Furthermore, the peak at 783 cm^{-1} corresponds to the stretching of the C–Cl bond, the out-of-plane motion of the C–H bond, the S-OR ester group, and the wagging motion of the N–H bond in amines. The signal at 1321 cm^{-1} indicates the presence of aromatic –H, aromatic C–C stretching, =CH out of the plane, and C–H bending in damaged samples. The peak at 678 cm^{-1} corresponds to the stretching of C–C bonds and the stretching of aromatic Ar–H bonds. Hence, the FTIR spectra of both the original and degraded RG12 samples, obtained after decolorization, confirmed the breakdown of azo dyes. Furthermore, the spectra obtained at the 4th, 8th, and 12th hours provided additional evidence of the progressive degradation of RG12 due to bacterial treatments (Fig. 4 b, c, d).

Phytotoxic effect of degraded and undegraded dye

The seeds of *Triticum aestivum* exposed to the parent dye (200 mg/mL) without any treatment showed a germination rate of 70%, indicating the presence of dye toxicity. On the

Table 1 Distinct peaks of spectra, peak wavelengths, and probable functional groups of parent and degraded Reactive Green 12 textile dye obtained after FTIR analysis

Peak number	Peak wavelength (cm ⁻¹)	Probable functional groups
<i>Parent Reactive Green 12 dye (Undegraded)</i>		
1	3738	Water OH stretch
2	3854	O–H stretching vibration
3	3325	C–H stretch, RCO–OH (dimer OH), NH stretch in amines, Ar O–H in phenol
4	2361	Carboxylic acid O–H stretch
5	2132	C≡C stretching for alkyl substituted, R–N–C isocyanide, N=C stretch in R–N=C=S, N=N=N stretching
6	1620	–N≡N– stretching, NH out of the plane, C=O stretch, NH ₂ in the plane band, C=N stretch, Ar–CH=CHR
7	1450	Azo group (–N=N–) stretch
8	585	C–Br stretch
<i>Treated Reactive Green 12 dye (Degraded)</i>		
1	3305	C–H stretching
2	3307–3419	N–H and O–H stretching
3	2123	C=C stretch, N=C in R–N=C=S
4	2123–24	Aromatic/aliphatic iso-nitrile (–N≡C–) stretching or possible azide stretching
5	2621, 2867, 2923	C–H stretching vibrations of aldehyde and alkane
6	1634–1637	Aromatic/aliphatic nitro compound (NO ₂) asymmetric stretching, Oxime stretching (C=N–OH)
7	1206	Stretching in phenols and also for N–H deformation in bonded N–H
8	1637	C=C stretch, NH out of the plane, C=O stretch, NH ₂ in-plane bend, C=N, N–H deformation
9	1139	CN stretching
10	783	C–Cl stretch, C–H out of the plane, S–OR ester, N–H wag amines
11	703	CS stretching of Sulphur containing compound
12	671–675	C–S stretching
13	686, 690	Aromatic C–H out of plane bending
14	692	Ar–H stretch, Ar C–C stretch, =CH out of the plane, NH stretch, C–H bend
15	678	C–C stretch, Ar–H stretch

other hand, the seeds treated with deteriorated dye samples displayed a 100% germination rate over a period of 5 days and did not show any signs of toxicity, which indicated a loss in toxicity of parent dye after treatments. In addition, the treatment of seeds with distilled water also did not show any toxic effect, and seeds germinated 100% and grew properly. Furthermore, the untreated dye solution resulted in a significant decrease in both the size of the plumule and the total number of roots in the germinated seeds. The size of the plumule in untreated seeds was significantly less (0.5 cm) compared to the treated seeds, which was 6.00 cm in length. The shoot length, root length, shoot vigor index, fresh weight, and dry weight of plants in the treated dye sample were measured to be 8.0, 4.5 cm, 1950, 1.37, and 0.38 g, respectively. In contrast, the sets treated with the untreated dye did not exhibit any growth or vegetative growth (Fig. 5, Table 2). Consequently, the observations of the shoot, root length, shoot vigor index, dry weight, and wet weight in both treated and untreated samples demonstrated a substantial impact of toxicity, resulting in no growth. Therefore, it was evident that the phytotoxicity experiment

findings demonstrated the capability of the isolated *B. cereus* SSC to both decolorize RG12 and detoxify it.

Genotoxic effect of degraded and undegraded dye

Chromosomal aberration was seen in the roots of *A. cepa* that were treated with the degraded dye. Multiple genotoxic lesions, characterized by chromosomal anomalies, were observed during the metaphase of cell division, as clearly depicted in the images (Fig. 6).

The chromosomal abnormalities detected in the cells of *A. cepa* root tips exposed to parent RG12 dye and degraded metabolites are depicted in Fig. 7e–h and a–d, respectively. The chromosomal abnormalities detected in root cells exposed to the dye included chromosome breakage, multipolar anaphase, irregular prophase, binucleated cells, aberrant metaphase, and chromosome bridges (Fig. 7e–h). The presence of aberrant metaphases was observed as the most common anomaly in all cells that were exposed to dye at doses of 0.5 mg/mL. Chromosome bridges, resulting from inefficient replication of chromosomes, have been observed

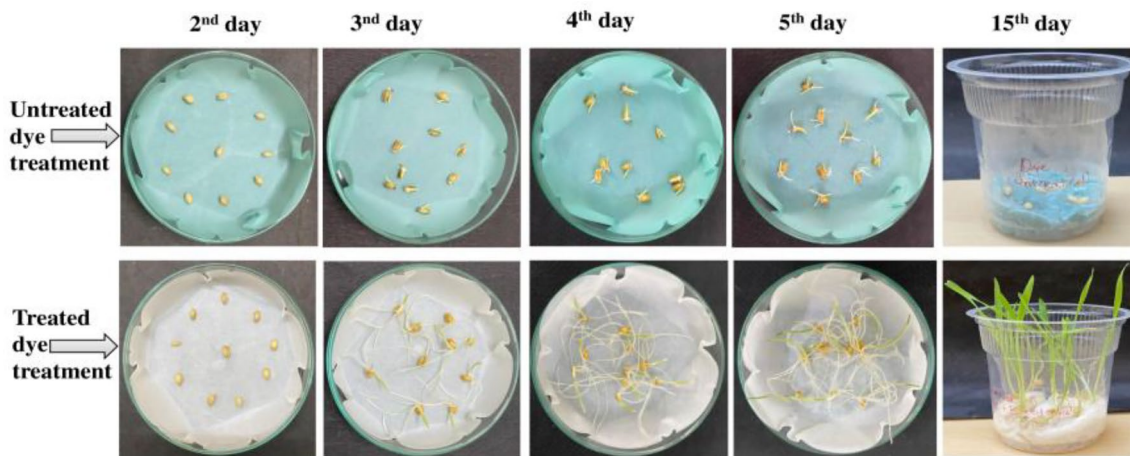


Fig. 5 Phytotoxicity assay of wheat (*Triticum aestivum*) seeds exposed with the treated and untreated dye samples

Table 2 Different parameters of the germination of *Triticum aestivum* seeds exposed to treated and untreated dye samples

Parameters	Treatment of seeds with the dye samples	
	Untreated dye	Treated dye
Germination (%)	70 ± 1.0	100 ± 0.62
Plumule (cm)	0.5 ± 0.62	6 ± 0.6
Number of roots	2	9
Shoot length (cm)	nd	8 ± 0.09
Length of root(cm)	nd	4.5 ± 0.72
Shoot vigor index	nd	1950
Fresh weight of plant (g)	nd	1.37 ± 0.9
Dry weight of plant (g)	nd	0.38 ± 0.6

± ; standard deviation (n = 3)

nd not detected



Fig. 6 Treatment of onion (*Allium cepa*) roots with the exposure of parent Reactive Green 12 dye and degraded dye solution

in cells treated with RG12 dye. The cells that were exposed to RG12 exhibited the characteristics of having two nuclei, which were likely a result of multipolar spindles (Fig. 7h). However, slight deviations without any chromosomal abnormalities were observed in all the cells exposed to the degraded metabolites (Fig. 7a–d).

Discussion

Employing microbes to biodegrade synthetic and carcinogenic colors has proven to be a promising biological and eco-friendly method over traditional treatments. The potential and capability of new microbes as important agents in pollution treatment have been ensured by their increased activity and expanded substrate specificity. The promising microbiological methods perform to be more effective in fully mineralizing and detoxifying the highly toxic and colored textile dyes. However, the concentration of dye is considered to be a critical variable that influences the effectiveness of decolorization by organisms. The present investigation found that *B. cereus* SSC demonstrated the most effective decolorization at a dye concentration of 200 mg/L. As the concentration of dye was progressively increased from 50 to 1000 mg/L, the efficiency of dye decolorization declined. Similar to the findings of the present investigation, publications indicate that the efficacy of decolorization reduced progressively as the concentration of dye increased (El-Bendary et al. 2023). In a study conducted by Jamee and Siddique (2019), it was shown that the rate of decolorization decreased gradually as the concentration of dye increased. The decline in phenomena may be attributed to either the harmful impact of the dye on bacterial cells or the improper binding of dye molecules with the active sites of degrading enzymes (El-Bendary

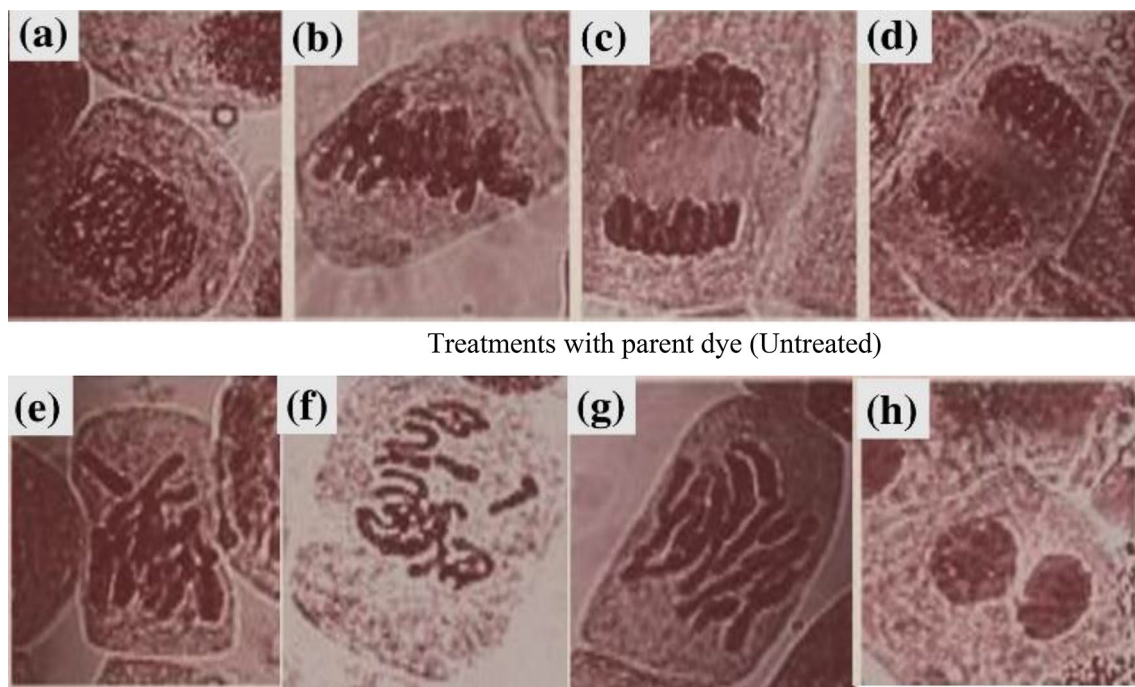


Fig. 7 Cytotoxic damages observed in meristematic cells of *A. cepa* roots exposed with parent Reactive Green 12 dye: **e** chromosome breaks at metaphase, **f** abnormal metaphase, **g** chromosome missegregation **h** binucleated and degraded: **a–d** cells with normal metaphase

et al. 2023). Zhuang et al. (2020) reported that an intrinsic toxicity of higher dye concentration was found to block the active sites of dye-degrading enzymes, inhibiting bacterial activity and degradation potential. It was recorded that the degradation of dye rises as dye concentration drops, and conversely, it reduces as dye concentration increases. Moreover, it was also observed that the static conditions favored the degradation of the RB12 dye. Similar results have also been demonstrated by Emadi et al. (2021). The decolorization of dyes happens by the action of the azoreductase enzyme under microaerophilic and anaerobic environments. This enzyme breaks the azo linkages of dyes, resulting in the formation of colorless molecules (Emadi et al. 2021; Khan et al. 2014). A similar incidence of enzymatic degradation of dye under static conditions with lesser oxygen might have also occurred in our study.

The HPLC is a highly effective device for assessing the biodegradation of chemical compounds (Thanavel et al. 2020). Tahir and Yasmin (2021) utilized HPLC to assess the rate of conversion and breakdown of Mordant Black 11 (MB11) dye into different metabolites. The HPLC analysis revealed the presence and absence of peaks in samples that were incubated for 4, 8, and 12 h, providing evidence for the breakdown of the dye by the *B. cereus* SSC strain. Bera and Tank (2021) consistently observed the formation of three prominent peaks at retention times of 2.600, 2.981, and 3.439 min in the treated sample. Additionally, they detected three smaller peaks at retention times of 4.654, 5.458, and

8.003 min (Bera and Tank 2021). Similarly, *Enterobacter hormaechei* SKB16 produced several degraded metabolites from the degradation of Reactive Red 198 (RR198). These metabolites were characterized by a large peak at 3.099 min and four smaller peaks at 3.425, 3.667, 5.275, and 6.051 min (Thangaraj et al. 2021). Thangaraj et al. (2021) found that *Enterobacter hormaechei* SKB16 produced degraded metabolites when RR198 was broken down. These metabolites were characterized by one major peak at 3.099 min and four minor peaks at 3.425, 3.667, 5.275, and 6.051 min. The appearance of additional peaks in the deteriorated dye indicates the decomposition of a large and complex parent dye into smaller and more basic components. In an identical manner, Tahir and Yasmin (2021) observed certain metabolites of Mordant Black 11 dye through the elution peak of the dye, which occurred at 5.045 min before any bacterial processing took place. In the bacterially treated samples, a new peak emerged at 4.556 min. The peaks were accompanied by different retention times. The confirmation of the breakdown of the dye into various metabolites is evidenced by a substantial shift in the primary peak of both the original dye and the degraded dye. In addition, the results of another study conducted by Buthelezi et al. in 2012 provided more support for the results and findings of the current investigation.

The FTIR analysis conducted in this study revealed that the deteriorated sample displayed a greater number of peaks compared to the original dye sample. The prominent peaks observed in the original dye samples were conspicuously

lacking in the deteriorated samples. Furthermore, the emergence of many new peaks, which suggest the existence of extra functional groups, was detected. Several peaks, specifically at 3307, 3349, and 3419 cm^{-1} , which correspond to the stretching of N–H and O–H bonds, were seen in the samples subjected to treatments lasting 4, 8, and 12 h. Additionally, a peak at 1634–37 cm^{-1} was also identified. In the investigation conducted by Prasad and Rao (2014), it was discovered that the treatment of *Aeromonas* sps. resulted in the highest values of 1618.28 and 1570.06 cm^{-1} for the C=C stretching in Acid Black-24 dye. Ayaz et al. (2015) showed that when acid blue 113 was analyzed using FTIR before and after being degraded by *Staphylococcus aureus* and *Escherichia coli*, distinct peaks were observed in the untreated dye. These peaks indicated stretching of N–H amine or O–H and aromatic =C–H at 3440 cm^{-1} . According to Telke et al. (2010), the decolorized product's FTIR pattern comparison shows that a peak at 1450 cm^{-1} has disappeared, indicating the absence of the (–N=N–) azo bond. Similar results were found by Telke et al. (2010) for the elimination of peaks during the investigation of *Aspergillus ochraceus* NCIM-1146 Blue Laccase's biochemical characterization and efficiency dye degradation. In addition, Emadi et al. (2022) reported that the absence of the peak corresponding to the biotransformed metabolites indicates that the azo linkages were broken down during the breakdown process of AB-113. This might indicate that the dye underwent degradation and developed new peaks. The changes in the peaks were most likely influenced by the modifications in the molecular structure of Reactive Black 5 (RB5). These modifications include the degradation of its main chromophores, the breaking of the –N=N– bond, the formation of amino groups, the appearance of additional intermediate metabolites, and the decomposition of RB5 during the process of dye decolorization (Emadi et al. 2022; Al-Tohamy et al. 2020; Dafale et al. 2008). The decrease in the highest levels of intensity in the low-frequency band of spectra (620–850 cm^{-1}) suggested the division of aromatic rings (Kolekar and Kodam 2012), which has also been observed in the present work. Al-Tohamy et al. (2020) discovered that *Salsuginibacillus halophiles* SSA1575 effectively degraded the chemical structure of RB5 during the decolorization process. The removal of these peaks clearly indicated the breakdown or deletion of the relevant bonds in the MR dye (Hu et al. 2021). A comparison was made between the FTIR spectra of the original dye and those of the degraded dye or metabolites. The analysis revealed notable differences between the two. After undergoing degradation, new peaks appeared while the original peaks of the methyl red disappeared, indicating a conversion into different compounds or metabolites. Ikram et al. (2022) showed through FTIR investigations that the azo bond in the Methyl Red (MR) dye was eliminated and reduced. In addition, the treated sample

showed a complete absence of hazardous substances, thus clearly demonstrating the mineralization of the dye.

The results of the phytotoxicity test showed that the seeds had a germination rate of 70% when exposed to a concentration of 200 mg/L of RG12 dye. However, when the seeds were exposed to the degraded dye sample, a germination rate of 100% was observed. Previous studies also demonstrated the inconsistent influence of artificial colors and their changing concentrations on the process of seed germination in many plant species, including *Triticum aestivum*, *Vigna radiata*, *Vigna aconitifolia*, *Vigna sinensis*, and *Cicer arietinum*. The investigation indicated that when the quantity of dye increased, it hindered the germination percentage of all plants (Ergene et al. 2009; Jadhav et al. 2016). Thangaraj et al. (2021) also reported similar results, showing significant toxicity with low germination rates of 10 and 23.3% following exposure to the parental dyes RR198 and Reactive Yellow 145 (RY145), respectively. Studies also reveal that degraded dye metabolites may also be toxic. Emadi et al. (2021, 2022) reported that the parent form of RB5 dye was not toxic and poisonous, but their degraded metabolites were found to be toxic, and because of toxicity, maize seeds were not germinated. However, in our study, parent dye was found to be toxic while degraded showed no toxicity and gave complete (100%). However, dye degraded by *Enterobacter hormaechei* SKB16 demonstrated higher seed germination rates, with 100% germination rate and growth of radical lengths 2.3 and 2.0 cm, respectively, for RR198 and RY145 dyes (Thangaraj et al. 2021). In contrast to the observations, the application of parent RG12 dye did not result in germination, possibly due to the higher toxicity of the untreated dye. Furthermore, Kurade et al. (2016) discovered that the metabolites generated from the decolorization process of Dispersed Red (DR54) dye utilizing *Bacillus laterosporus* were proven to be non-toxic, therefore indicating successful detoxification of the DR54 dye. This demonstrates that the samples subjected to treatment do not have any harmful effect on the growth of the plants under study. The study found that the destroyed dye metabolites did not harm plant growth, suggesting that water cleared by the bacterium is suitable for irrigation without any safety concerns (Fareed et al. 2022). After the dye was decolorized and degraded, the germination rate increased to more than 90% when metabolites were present (Amin et al. 2020). Hence, the results of this investigation further validated the harmless characteristics of the dye's degraded metabolites obtained from RG12 dye and the bacteria *B. cereus* SSC, suggesting their possible application in dye degradation. The findings given above provide clear evidence that the dye has undergone thorough mineralization and detoxification (Bera and Tank 2021).

An examination of chromosomal aberrations in the meristematic root tip cells of *A. cepa* is considered a valuable test for assessing the genetic toxicity potential of pesticides,

sewage, and industrial wastewaters (Grover and Kaur 1999; Leme and Marin-Morales 2009; Radic et al. 2010; Haq et al. 2016). The normal cells did not exhibit any chromosomal aberrations or nuclear abnormalities. Chromosomal abnormalities, such as chromosome breakage, irregular prophase, chromosome bridges, multipolar anaphase, binucleated cells, and aberrant metaphase, were observed in cells that were exposed to parent dye. Important abnormalities that need to be addressed include structural abnormalities in chromosomes, such as bridges, breaks, and loss, as well as delays in chromosomal replication, adhesion, and the presence of many poles. These abnormalities are caused by aneugenic agents, as discussed by Leme and Marin-Morales in 2009. This phenomenon could be attributed to the interactions or inhibitions of vital structures involved in the formation of the mitotic spindle, which obstructs the advancement of cell division and results in chromosomal abnormalities (Castro et al. 2021). Furthermore, meristematic root cells that are exposed to toxic wastewater exhibit a range of chromosomal abnormalities, such as multipolar anaphase, vragrant chromosome, anaphase with chromosome break, disrupted metaphase, and lagging chromosome (Puvanewari et al. 2006)—evaluation of toxicity and microbiological breakdown of azo dyes. Jadhav et al. (2011) reported that the amount and frequency of anomalies decreased through the process of dye biodegradation. Previous studies have also confirmed the presence of a comparable form of genotoxicity in textile effluents (Carita and Marin-Morales 2008; Jadhav et al. 2010).

Conclusion

In conclusion, the bacterial strain *B. cereus* SSC demonstrated exceptional efficiency in decolorizing and degrading the RG12 dye within 12 h, achieving a remarkable 97.8% decolorization of 200 mg/L dye. Analyses through HPLC and FTIR revealed a significant reduction in absorption levels, with distinct differences in the FT-IR spectra between the original dye and its metabolites, showing varied peaks at different wavelengths. The bacterial degradation was evident from the loss of azo linkages ($-N=N-$). The HPLC analysis displayed fluctuations in peaks and retention times, indicating dye degradation. *B. cereus* SSC effectively converted RG12 into non-toxic byproducts, as confirmed by 100% seed germination and healthy plant growth in a phytotoxicity assay. Furthermore, genotoxicity experiments on *Allium cepa* cells, too, showed no adverse effects from the degraded dye, affirming the successful elimination of the dye. Therefore, according to the findings of this study, the newly examined bacterial strain can be utilized in the process of bioremediation and detoxification of textile dyes. Consequently, we strongly advocate for the use of bacterial

inoculum for the remediation and detoxification of textile contaminants. Further, it is also recommended that degraded and detoxified dye wastewater be recycled for the irrigation of agricultural crops.

Acknowledgements The authors are highly thankful to Cytogene Laboratory, Lucknow (UP), India, for helping in the HPLC and FTIR analysis.

Author contributions SS Performed analyses of the study. RLG performed the writing. DC & DS Reviewed and analyzed the data. RN Conceptualized the study and critically reviewed the experiments during the entire study.

Funding This research received no external funding.

Data availability No datasets were generated or analyzed during the current study.

Declarations

Conflict of interest The authors confirm that they have no competing financial interests or personal relationships that could have potentially influenced the work presented in this study.

References

- Alsukaibi AK (2022) Various approaches for the detoxification of toxic dyes in wastewater. *Processes* 10(10):1968. <https://doi.org/10.3390/pr10101968>
- Al-Tohamy R, Kenawy E, Sun J, Ali SS (2020) Performance of a newly isolated salt-tolerant yeast strain *Sterigmatomyces halophilus* SSA-1575 for azo dye decolorization and detoxification. *Front Microbiol* 11:1163. <https://doi.org/10.3389/fmicb.2020.011163>
- Amin S, Rastogi RP, Chaubey MG, Jain K, Divecha J, Desai C, Madamwar D (2020) Degradation and toxicity analysis of a reactive textile diazo dye-Direct red 81 by newly isolated bacillus sp. DMS2. *Front Microbiol* 11:576680. <https://doi.org/10.3389/fmicb.2020.576680>
- Ayaz N, Thankappan R, Srinivasan SV, TamilSelvi A (2015) Studies on decolorisation of Acid Blue 113 using *Staphylococcus aureus* and *Escherichia coli* isolated from tannery wastewater. *Int J Innov Res Sci Eng Technol* 4(3):938–948
- Bharti V, Vikrant K, Goswami M, Tiwari H, Sonwani RK, Lee J, Tsang DC, Kim KH, Saeed M, Kumar S, Rai BN (2019) Biodegradation of methylene blue dye in a batch and continuous mode using biochar as packing media. *Environ Res* 171:356–364. <https://doi.org/10.1016/j.envres.2019.01.051>
- Bholay A, Borkhataria BV, Jadhav PU, Palekar KS, Dhalkari MV, Nalawade P (2012) Bacterial lignin peroxidase: a tool for biobleaching and biodegradation of industrial effluents. *Univ J Environ Res Technol* 2:58–64
- Bilinska L, Blus K, Gmurek M, Ledakowicz S (2019) Coupling of electrocoagulation and ozone treatment for textile wastewater reuse. *Chem Eng J* 358:992–1001. <https://doi.org/10.1016/j.cej.2018.10.093>
- Buntić AV, Pavlović MD, Antonovic DG, Siler-Marinković SS, Dimitrijević-Branković SI (2017) A treatment of wastewater containing basic dyes by the use of new strain *Streptomyces microflavus* CKS6. *J Clean Prod* 148:347–354. <https://doi.org/10.1016/j.jclepro.2017.01.164>
- Buthlezi SP, Olaniran AO, Pillay B (2012) Textile dye removal from wastewater effluents using biofloculants produced by indigenous

- bacterial isolates. Mole 17(12):14260–14274. <https://doi.org/10.3390/molecules171214260>
- Cao J, Sanganyado E, Liu W, Zhang W, Liu Y (2019) Decolorization and detoxification of Direct Blue 2B by indigenous bacterial consortium. J Environ Manage 242:229–237. <https://doi.org/10.1016/j.jenvman.2019.04.067>
- Caritá R, Marin-Morales MA (2008) Induction of chromosome aberrations in the *Allium cepa* test system caused by the exposure of seeds to industrial effluents contaminated with azo dyes. Chemosphere 72(5):722–725. <https://doi.org/10.1016/j.chemosphere.2008.03.056>
- Dafale N, Rao NN, Meshram SU, Wate SR (2008) Decolorization of azo dyes and simulated dye bath wastewater using acclimatized microbial consortium biostimulation and halo tolerance. Bioreour Technol 99(7):2552–2558. <https://doi.org/10.1016/j.biortech.2007.04.044>
- Dagar S, Singh SK, Gupta MK (2022) Economics of advanced technologies for wastewater treatment: evidence from pulp and paper industry. Front Environ Sci 10:960639. <https://doi.org/10.3389/fenvs.2022.960639>
- D'Souza E, Fulke AB, Mulani N et al (2017) Decolorization of Congo red mediated by marine *Alcaligenes* species isolated from Indian West coast sediments. Environ Earth Sci 76:721. <https://doi.org/10.1007/s12665-017-7077-8>
- El-Bendary MA, Fawzy ME, Abdelraof M, El-Sedik M, Allam MA (2023) Efficient malachite green biodegradation by *Pseudomonas plecoglossicida* MG2: process optimization, application in bioreactors, and degradation pathway. Microb Cell Fact 22:192. <https://doi.org/10.1186/s12934-023-02194-z>
- Emadi Z, Sadeghi R, Forouzandeh S, Mohammadi-Moghadam F, Sadeghi R, Sadeghi M (2021) Simultaneous anaerobic decolorization/degradation of Reactive Black-5 azo dye and chromium (VI) removal by *Bacillus cereus* strain MS038EH followed by UV-C/H₂O₂ post-treatment for detoxification of biotransformed products. Arch Microbiol 203:4993–5009. <https://doi.org/10.1007/s00203-021-02462-9>
- Ergene A, Ada K, Tan S, Katircioğlu HJ (2009) Removal of Remazol Brilliant Blue R dye from aqueous solutions by adsorption onto immobilized *Scenedesmus quadricauda*: Equilibrium and kinetic modeling studies. Desalination 249:1308–1314. <https://doi.org/10.1016/j.desal.2009.06.027>
- Fareed A, Zaffar H, Bilal M, Hussain J, Jackson C, Naqvi TA (2022) Decolorization of azo dyes by a novel aerobic bacterial strain *Bacillus cereus* strain ROC. PLoS ONE 17(6):e0269559. <https://doi.org/10.1371/journal.pone.0269559>
- Forss J, Lindh MV, Pinhassi J, Welander U (2017) Microbial biotreatment of actual textile wastewater in a continuous sequential rice husk biofilter and the microbial community involved. PLoS ONE 12(1):e0170562. <https://doi.org/10.1371/journal.pone.0170562>
- Garg N, Garg A, Mukherji S (2020) Eco-friendly decolorization and degradation of reactive yellow 145 textile dye by *Pseudomonas aeruginosa* and *Thiosphaera pantotropha*. J Environ Manage 263:110383. <https://doi.org/10.1016/j.jenvman.2020.110383>
- Goud BS, Cha HL, Koyyada G, Kim JH (2020) Augmented biodegradation of textile azo dye effluents by plant endophytes: a sustainable, eco-friendly alternative. Curr Microbiol 77(11):3240–3255. <https://doi.org/10.1007/s00284-020-02202-0>
- Grover IS, Kaur S (1999) Genotoxicity of wastewater samples from sewage and industrial effluent detected by the *Allium* root anaphase aberration and micronucleus assays. Mutat Res 426(2):183–188. [https://doi.org/10.1016/s0027-5107\(99\)00065-2](https://doi.org/10.1016/s0027-5107(99)00065-2)
- Guendouz S, Khellaf N, Zerdaoui M, Ouchefoun M (2013) Biosorption of synthetic dyes (Direct Red 89 and Reactive Green 12) as an ecological refining step in textile effluent treatment. Environ Sci Pollut Res Int 20(6):3822–3829. <https://doi.org/10.1007/s11356-012-1314-1>
- Hu CY, Cheng HY, Yao XM, Li LZ, Liu HW, Guo WQ, Fu JL (2021) Biodegradation and decolorization of methyl red by *Aspergillus versicolor* LH1. Prep Biochem Biotech 51(7):642–649. <https://doi.org/10.1080/10826068.2020.1848868>
- Ikram M, Naeem M, Zahoor M, Rahim A, Hanafiah MM, Oyekanmi AA, Shah AB, Mahnashi MH, Al Ali A, Jalal NA et al (2022) Biodegradation of Azo Dye Methyl Red by *Pseudomonas aeruginosa*: Optimization of process conditions. Int J Environ Res Public Health 19:9962. <https://doi.org/10.3390/ijerph19169962>
- Jadhav SB, Phugare SS, Patil PS, Jadhav JP (2011) Biochemical degradation pathway of textile dye Remazol red and subsequent toxicological evaluation by cytotoxicity, genotoxicity, and oxidative stress studies. Int Biodeterior Biodegrad 65(6):733–743. <https://doi.org/10.1016/j.ibiod.2011.04.003>
- Jadhav U, Dhawale R, Dawkar V, Chougale A, Padul M (2016) Phytotoxic effect of synthetic textile dye effluent on growth of five plant species. Trends Biotech Res 5:1–6
- Jamee R, Siddique R (2019) Biodegradation of synthetic dyes of textile effluent by microorganisms: an environmentally and economically sustainable approach. Eur J Microbiol Immunol 9(4):114–118. <https://doi.org/10.1556/1886.2019.00018>
- Kalyani DC, Telke AA, Govindwar SP, Jadhav JP (2009) Biodegradation and detoxification of reactive textile dye by isolated *Pseudomonas* sp. SUK1. Water Environ Res 81(3):298–307. <https://doi.org/10.2175/106143008x357147>
- Khan Z, Jain K, Soni A, Madamwar D (2014) Microaerophilic degradation of sulphonated azo dye—Reactive Red 195 by bacterial consortium AR1 through co-metabolism. Int Biodeter Biodegrad 94:167–175
- Khan MK, Babar SF, Oryani B, Dagar V, Rehman A, Zakari A et al (2022) Role of financial development, environmental-related technologies, research and development, energy intensity, natural resource depletion, and temperature in sustainable environment in Canada. Environ Sci Pollut Res 29(1):622–638. <https://doi.org/10.1007/s11356-021-15421-0>
- Kishor R, Purchase D, Saratale GD, Ferreira LF, Bilal M, Iqbal HM, Bharagava RN (2021) Environment-friendly degradation and detoxification of Congo red dye and textile industry wastewater by a newly isolated *Bacillus cohnii* (MW406977). Environ Technol Inno 22:1–26. <https://doi.org/10.1016/j.eti.2021.101425>
- Kolekar YM, Kodam KM (2012) Decolorization of textile dyes by *Alishewanella* sp KMK6. Appl Microbiol Biotechnol 95:521–529. <https://doi.org/10.1007/s00253-011-3698-0>
- Krishnamoorthy R, Jose PA, Ranjith M, Anandham R, Suganya K, Prabhakaran J, Thiyaageshwari S, Johnson J, Gopal NO, Kumutha K (2018) Decolourisation and degradation of azo dyes by mixed fungal culture consisted of *Dichotomomyces cejpji* MRCH 1–2 and *Phoma tropica* MRCH 1–3. J Environ Chem Eng 6(1):588–595. <https://doi.org/10.1016/j.jece.2017.12.035>
- Kumaran S, Ngo ACR, Schultes FP, Saravanan VS, Tischler D (2022) In vitro and in silico analysis of Brilliant Black degradation by *Actinobacteria* and a *Paraburkholderia* sp. Genomics 114(2):110266. <https://doi.org/10.1016/j.ygeno.2022.01.003>
- Padamavathy S (2003) Aerobic decolorization of reactive azo dyes in presence of various cosubstrates. Chem Biochem Eng Q 17:147–152
- Pandey A, Singh P, Iyengar L (2007) Bacterial decolorization and degradation of azo dye. Int Biodeterior Biodegrad 59:73–84. <https://doi.org/10.1016/j.ibiod.2006.08.006>
- Parshetti GK, Telke AA, Kalyani DC, Govindwar SP (2010) Decolorization and detoxification of sulphonated azo dye methyl orange by *Kocuria rosea* MTCC 1532. J Hazard Mater 176:503–509. <https://doi.org/10.1016/j.jhazmat.2009.11.058>
- Peng H, Guo J (2020) Removal of chromium from wastewater by membrane filtration, chemical precipitation, ion exchange, adsorption electrocoagulation, electrochemical reduction,

- electrodialysis, electrodeionization, photocatalysis and nanotechnology: a review. *Environ Chem Lett* 18:2055–2068. <https://doi.org/10.1007/s10311-020-01058-x>
- Prasad AS, Rao KV (2013) Aerobic biodegradation of Azo dye by *Bacillus cohnii* MTCC 3616; an obligately alkaliphilic bacterium and toxicity evaluation of metabolites by different bioassay systems. *Appl Microbiol Biotechnol* 97(16):7469–7481. <https://doi.org/10.1007/s00253-012-4492-3>
- Prasad AA, Rao KB (2014) Aerobic biodegradation of azo dye Acid Black-24 by *Bacillus halodurans*. *J Environ Biol* 35(3):549
- Puvanewari N, Muthukrishnan J, Gunasekaran P (2006) Toxicity assessment and microbial degradation of azo dyes. *Indian J Exp Biol* 44(8):618–626
- Qin XD, Zhu ZW, Liu G, Fu HM, Zhang HW, Wang AM, Li H, Zhang HF (2016) Ultrafast degradation of azo dyes catalyzed by cobalt-based metallic glass. *Sci Rep* 5:18226. <https://doi.org/10.1038/srep18226>
- Radic S et al (2010) The evaluation of surface and wastewater genotoxicity using the *Allium cepa* test. *Sci Total Environ* 408(5):1228–1233. <https://doi.org/10.1016/j.scitotenv.2009.11.055>
- Rao KB, Prasad AA (2014) Biodecolourisation of azo dye reactive red 22 by *Bacillus infantis* strain AAA isolated from seawater and toxicity assessment of degraded metabolites. *Nature Environ Poll Technol* 13(2):369
- Ryu S, Park YK, Shim J, Lim S, Kim M (2023) Highly sustainable dyes adsorption in wastewater using textile filters fabricated by UV irradiation. *Polymers (Basel)* 16(1):15. <https://doi.org/10.3390/polym16010015>
- Sabeen M, Mahmood Q, Bhatti ZA, Irshad M, Bilal M, Hayat MT, Shahid N (2020) *Allium cepa* assay based comparative study of selected vegetables and the chromosomal aberrations due to heavy metal accumulation. *Saudi J Biol Sci* 27(5):1368–1374. <https://doi.org/10.1016/j.sjbs.2019.12.011>
- Singh P, Srivastava N, Singh P, Geetha S, Usharani N, Jagadish RS, Upadhyay A (2019) Effect of toxic pollutants from pulp and paper mill on water and soil quality and its remediation. *Int J Lakes Rivers* 12(1):1–20
- Singh A, Pal DB, Mohammad A, Alhazmi A, Haque S, Yoon T, Srivastava N, Gupta VK (2022) Biological remediation technologies for dyes and heavy metals in wastewater treatment: New insight. *Bioresour Technol* 343:126154. <https://doi.org/10.1016/j.biortech.2021.126154>
- Telke AA, Kadam AA, Jagtap SS, Jadhav JP, Govindwar SP (2010) Biochemical characterization and potential for textile dye degradation of blue laccase from *Aspergillus ochraceus* NCIM-1146. *Biotechnol Bioprocess Eng* 15:696–703. <https://doi.org/10.1007/s12257-009-3126-9>
- Thanavel M, Bankole PO, Selvam R, Govindwar SP, Sadasivam SK (2020) Synergistic effect of biological and advanced oxidation process treatment in the biodegradation of Remazol yellow RR dye. *Sci Rep* 10(1):20234. <https://doi.org/10.1038/s41598-020-77376-5>
- Thangaraj S, Bankole PO, Sadasivam SK (2021) Microbial degradation of azo dyes by textile effluent adapted, *Enterobacter hormaechei* under microaerophilic condition. *Microbiol Res* 250:126805. <https://doi.org/10.1016/j.micres.2021.126805>
- Zhuang M, Sanganyado E, Zhang X, Xu L, Zhu J, Liu W, Song H (2020) Azo dye degrading bacteria tolerant to extreme conditions inhabit nearshore ecosystems: optimization and degradation pathways. *J Environ Manage* 261:110222. <https://doi.org/10.1016/j.jenvman.2020.110222>
- Bera SP, Tank SK (2021) Microbial degradation of Procion Red by *Pseudomonas stutzeri*. *Sci Rep* 11(1):3075. <https://doi.org/10.1038/s41598-021-82494-9>
- Castro ALG, Cruz JN, Sodré DF, Correa-Barbosa J, Azonsivo R, de Oliveira MS, Vale VV (2021) Evaluation of the genotoxicity and mutagenicity of isoeleutherin and eleutherin isolated from *Eleutherine plicata* herb. using bioassays and in silico approaches. *Arab J Chem* 14(4):103084. <https://doi.org/10.1016/j.arabjc.2021.103084>
- Emadi Z, Sadeghi M, Forouzandeh S, Sadeghi R, Sadeghi R, Mohammadi-Moghadam F (2022) Simultaneous decolorization/degradation of AB-113 and chromium (VI) removal by a salt-tolerant *Klebsiella* sp. AB-PR and detoxification of bio-transformed-metabolites. *Int J Environ Sci Technol* 19(3):2007–2024. <https://doi.org/10.1007/s13762-021-03360-9>
- Fazeliyan E, Sadeghi M, Forouzandeh S, Doosti A, Mohammadi Moghadam F, Sedehi M, Emadi Z, Sadeghi R (2021) Decolorization mechanism, identification of an FMN-dependent NADH-azoreductase from a moderately halotolerant *Staphylococcus* sp. MEH038S, and toxicity assessment of biotransformed metabolites. *Water Environ Res* 93(10):2072–2083. <https://doi.org/10.1002/wer.1580>
- Haq I, Kumari V, Kumar S, Raj A, Lohani M, Bhargava RN (2016) Evaluation of the phytotoxic and genotoxic potential of pulp and paper mill effluent using *Vigna radiata* and *Allium cepa*. *Adv Biol*:2356–6582. <https://doi.org/10.1155/2016/8065736>
- Hatice AE (2010) The handbook of environmental chemistry, biodegradation of azo dye, vol. 9. Springer, Berlin, Heidelberg, pp 39–57. https://doi.org/10.1007/978-2009_43
- Jadhav JP, Kalyani DC, Phugare SS, Govindwar SP (2010) Evaluation of the efficacy of a bacterial consortium for the removal of color, reduction of heavy metals, and toxicity from textile dye effluent. *Biores Technol*. <https://doi.org/10.1016/j.biortech.2009.08.027>
- Kishor R, Bharagava RN, Saxena G (2018) Industrial wastewaters: the major sources of dye contamination in the environment, ecotoxicological effects, and bioremediation approaches. In: Bharagava RN (ed) Recent advantage in environmental management. CRC Press Taylor & Francis, p13
- Kumaran S, Ngo ACR, Schultes FJP, Tischler D (2020) Draft genome sequence of *Kocuria indica* DP-K7, a methyl red degrading actinobacterium. *3 Biotech* 10:1–10. <https://doi.org/10.1007/s13205-020-2136-3>
- Kurade MB, Waghmode TR, Khandar RV, Jeon BH, Govindwar SP (2016) Biodegradation and detoxification of textile dye Disperse Red 54 by *Brevibacillus laterosporus* and determination of its metabolic fate. *J Biosci Bioeng* 121(4):442–449. <https://doi.org/10.1016/j.jbiosc.2015.08.014>
- Leme DM, Marin-Morales MA (2009) *Allium cepa* test in environmental monitoring: a review on its application. *Mutat Res Rev Mut Res* 682(1):71–81. <https://doi.org/10.1016/j.mrrev.2009.06.002>
- Rastogi S, Chaubey R P, Jain MG, Divecha K, Desai J, Madamwar C, Madamwar D (2020) Degradation and toxicity analysis of a reactive textile diazo dye-Direct Red 81 by newly isolated *Bacillus* sp. DMS2. *Front Microbiol* 11:576680. <https://doi.org/10.3389/fmicb.2020.576680>
- Sampaio AC, Bezerra RMF, Dias AA (2018) Mediterranean forested wetlands are yeast hotspots for bioremediation: a case study using azo dyes. *Sci Rep* 8:15943. <https://doi.org/10.1038/s41598-018-34325-7>
- Singh RP, Singh PK, Singh RL (2017) Role of azoreductases in bacterial decolorization of azo dyes. *Cur Trends Biomed Eng Biosci* 9:50–52. <https://doi.org/10.19080/CTBEB.2017.09.555764>
- Tahir U, Yasmin A (2021) Decolorization and discovery of metabolic pathway for the degradation of Mordant Black 11 dye by *Klebsiella* sp. MB398. *Braz J Microbiol* 52(2):761–771. <https://doi.org/10.1007/s42770-021-00470-x>

Publisher's Note Springer Nature remains neutral with regard to jurisdictional claims in published maps and institutional affiliations.

Springer Nature or its licensor (e.g. a society or other partner) holds exclusive rights to this article under a publishing agreement with the

author(s) or other rightsholder(s); author self-archiving of the accepted manuscript version of this article is solely governed by the terms of such publishing agreement and applicable law.